BIBECHANA
Vol. 23, No. 2, April 2026, 169-181

ISSN 2091-0762 (Print), 2382-5340 (Online)
Journal homepage: http://nepjol.info/index.php/BIBECHANA
Publisher:Dept. of Phys., Mahendra Morang A. M. Campus (Tribhuvan University)Biratnagar

Study of orientation of spin vectors of near infrared galaxies of low redshifted SDSS DR-19 Galaxies

Birendra Prasad Yadav, Shiv Narayan Yadav, Ajay Kumar Jha, Ram Chandra Devkota

Central Department of Physics, Tribhuvan University, Kirtipur, Kathmandu, Nepal.

*Corresponding authors: Email: shiva.yadav@cdp.tu.edu.com

Abstract

This study presents an analysis of the spatial orientations of 492,268 SDSS galaxies with redshifts ranging from 0.010 to 0.150, utilizing data from the 19th data release (DR19). The primary objective of this research is to investigate the nonrandom effects associated with the orientations of angular momentum in galaxies within the specified redshift range, evaluated through three distinct scenarios: the Hierarchy model, the Pancake model, and the Primordial Vorticity model. The analysis involves transforming the two-dimensional observational data—including positions, position angles, and inclination angles—into three-dimensional rotation axes characterized by polar and azimuthal angles. This transformation is accomplished using the position angle-inclination method. Our principal aim is to explore the relationship between spatial orientation and the z-magnitude in low-redshift galaxies. Expected isotropic distribution curves are generated by accounting for selection effects and conducting a random simulation that produces 10^7 virtual galaxies. To compare the observed and expected distributions, we employ four statistical tests: Chi-square analysis, Autocorrelation, First order Fourier Coefficient and first order Fourier Probability. An equatorial coordinate system has been selected as our reference; however, it is noteworthy that the observed preferred alignments are consistent regardless of the coordinate system employed. Despite this, localized anisotropies are evident in several samples, suggesting the potential influence of gravitational tidal interactions among neighboring galaxies and an early merging process that may alter the initial alignment of nearby galaxies. Specifically, samples z01, z02, z03, z04, z05, z06, z07, z10, z11, and z17 exhibit isotropy and remaining samples exhibit anisotropy in the polar angle (θ) distribution, while samples z01, z02, z03, z04, and z12 to z19 exhibit isotropy and remaining samples exhibit anisotropy in the azimuthal angle (ϕ) distribution. Some of the identified local anisotropies may be attributed to tidal interactions between galaxies or gravitational shearing effects, as indicated by previous studies. A follow-up multi-wavelength investigation is recommended to gain further insights into these phenomena.

Keywords
Coulomb stress, elastic rebound theory, slip, fault, Himalaya seismicity.

Article information
Manuscript received: February 3, 2026; Revised: April 19, 2026; Accepted: April 21, 2026
DOI https://doi.org/10.3126/bibechana.v23i2.92073

1 Introduction

The gravitational field distribution among galaxy constituents and their structural formation is a pivotal aspect in modeling. Over the years, numerous scenarios for galaxy formation have been proposed [1–6]. As new observational data become available, these scenarios undergo continuous refinement and adjustments [7,8], igniting considerable debate over how galaxies obtain their angular momentum, a characteristic that ultimately encompasses galaxy clusters and larger structures. The mechanism through which angular momentum is gained is intricately linked to the gravitational field distribution mentioned earlier. The currently accepted cosmological model is the spatially flat, homogeneous, and isotropic Cold Dark Matter (CDM) model.

In this framework, galaxy clusters form due to adiabatic and nearly scale-invariant Gaussian fluctuations [9–11]. This premise serves as the foundation for the hierarchical clustering model [1, 5], which is the most widely recognized scenario for galaxy formation. However, there also exist models that incorporate non-Gaussian initial fluctuations, although such non-Gaussianity has primarily been hypothesized rather than mathematically derived. Notably, non-Gaussian distributions can emerge from initial Gaussian distributions through the time evolution of galaxies, a process explained by solutions to Fokker-Planck equations with fractional derivatives [12, 13]. Consequently, initial Gaussian fluctuations may transform into non-Gaussian forms due to rapid early evolution, followed by a slower evolution characterized by the CDM scenario [14]. While the details of this primordial evolution are not addressed here, one of the objectives of this paper is to present a method for calculating non-Gaussian distribution functions derived solely from the interactions among astronomical objects. This distribution function represents the final outcome of the previously discussed rapid evolutionary process. According to the cosmological principle, the universe appears homogeneous and isotropic when observed on large scales [15]. Galaxy clusters, as significant gravitationally bound structures, provide valuable insights into the evolution of these aggregates, highlighting the necessity of understanding their formation, structural evolution, and the temporal changes in their constituents. The Lambda Cold Dark Matter (LCDM) model offers a coherent explanation for the large-scale structures of galaxy clusters and the distribution of light elements including hydrogen, helium, deuterium, and lithium [14]. In the context of hierarchical clustering, large-scale structures form from the interplay of gravitational interactions among their constituents. This indicates that smaller entities, such as galaxies, form first and later combine into larger structures. As a result, the angular momentum of galaxies arises from tidal interactions with their neighboring galaxies [16]. Initially, hierarchical clustering models suggested a completely random distribution of galaxy angular momenta. However, subsequent research has shown that the local tidal shear tensor can induce a local alignment of angular momenta within galaxies [17–19]. These mechanisms, known as tidal torque mechanisms, were first introduced by Hoyle [20] and later elaborated upon by White [21]. A review by Kiessling et al. [22] also addresses galaxy alignments in the context of gravitational lensing. In our model, angular momentum results from tidal interactions with the entire environment, with the effects of these interactions propagating from nearby to distant galaxies. This perspective refines the approaches previously suggested by Schäfer & Merkel [16], Catelan & Theuns [17], and Lee & Pen [18], which considered the "mean" tidal interaction across the environment as a whole. Conversely, the tidal torque mechanism is based on the Zeldovich pancake model, which posits that structures in the universe evolve from top to bottom [2–4].

In this framework, a magneto-hydrodynamic shock wave plays a crucial role, causing large structures to break apart. These shock waves arise from the asymmetrical collapse of an initial large structure, imparting angular momentum to galaxies. This model suggests a coherent, non-random spatial orientation of galaxy planes, with the rotational axes of galaxies aligning in parallel to the primary plane of a large structure. In the primordial turbulence model, the angular momentum of galaxies is believed to be a remnant of early cosmic vortex phenomena [23–25]. This indicates that galaxies' rotational axes exhibit a non-random orientation, with their preferred direction of angular momentum being perpendicular to the main plane of a large structure. Gamow [26], Gödel [27], and later Collins & Hawking [28] noted that if the universe rotates, the angular momentum of newly formed galaxies arises from the conservation principles of a rotating universe. However, it has been argued against this notion that such a model predicts a specific alignment of galaxy rotational axes that has not been corroborated by observational evidence [29]. It is essential to emphasize that the assumption that each of the aforementioned approaches (primordial turbulence, hierarchical clustering, and Zeldovich pancakes yields distinct orientations for galaxy axes

is overly simplistic. Each model, including hierarchical clustering, may involve phases characterized by shock waves typically linked to structural or substructural collapses [7, 30, 31], which could potentially lead to organized rotational axes. The scale of such organization may differ among various models. For instance, Bower's scenario [32] argues that hierarchical clustering does not occur uniformly across all mass scales. Instead, anti-hierarchical clustering emerges at smaller scales due to tidal interactions, resulting in Zeldovich pancake-like objects rather than spherically collapsing halos. Nonetheless, a critical distinction exists between the classical pancake scenario and anti-hierarchical clustering, as the latter is localized to small scales. The hierarchical clustering model remains distinctive for its explicit consideration of dark matter. The Li model initially treated the universe as a dust fluid, but it can also incorporate dark matter as a foundational element.

In this framework, dark matter interacts with observable matter only gravitationally. In contrast, the primordial turbulence and Zeldovich pancake models solely consider a dust component, leaving successful attempts to integrate dark matter unaddressed. Consequently, these two models are excluded from the ongoing discussion. Theoretical models of galaxy formation often encounter difficulties in explaining the observational correlation between angular momentum and structural mass. This correlation is evident only in two specific model classes: the tidal torque scenario [17, 33–35] and the Li model [36, 37]. Other models fail to establish such a dependence. It's important to note that the Li model necessitates a global or at least large-scale rotation of the universe. Li & Li-Xin [35] investigated the relationship between angular momentum and the mass of spiral galaxies, estimating the universe's rotation to be close to values reported by Birch [38]. However, this estimated value is excessively high in comparison to the observed anisotropy in the Cosmic Microwave Background Radiation (CMBR).

1.1 Data release 19

The Sloan Digital Sky Survey's (SDSS) Data Release 19 (DR19) marks a significant achievement in the continuous endeavor to chart the universe's structure and gain insights into the characteristics of astronomical objects. SDSS is widely recognized for its extensive multi-spectral imaging, spectroscopy, and photometry of celestial bodies. DR19 provides updated information on a diverse array of astronomical entities, including galaxies, quasars, stars, and beyond. This release boasts enhanced data processing, sophisticated algorithms, and a more comprehensive database that empowers researchers to explore cosmic phenomena more profoundly [39]. Here are some of the major highlights of SDSS DR19:

1.2 Expanded coverage

DR19 greatly increases the area of the night sky that has been surveyed, offering a richer dataset for current and upcoming astrophysical research.

1.3 Refined spectroscopy

Improved spectroscopic data are available for a wide variety of objects, enabling more accurate measurements of redshifts, chemical makeups, and other characteristics.

1.4 Advanced techniques

The techniques used for data processing have been enhanced to minimize systematic errors, thereby elevating the quality of astronomical measurements and leading to more credible scientific findings.

1.5 Transformation of coordinates

The Godlowskian transformation is a mathematical procedure used in observational astrophysics to convert two-dimensional (2D) projected data of galaxies into three-dimensional (3D) spatial information regarding their orientation. Specifically, it is used to calculate the 3D angular momentum vectors (spin vectors) of galaxies, allowing astronomers to analyze whether galaxies in a cluster or supercluster are aligned randomly or have preferred orientations.

The three-dimensional parameters θ (polar angle) and ϕ (azimuthal angle) can be obtained using Godlowskian Transformation of the position angle (p), inclination angle (i), right ascension (α) and declination (δ) are given in the Equations (1) and (2) [40].

$$\sin\theta = -\cos i\,\sin\delta \pm \sin i\,\sin P\,\cos\delta \tag{1}$$

$$\sin\phi = (\cos\theta)^{-1}\Big[-\cos i\cos\delta\sin\alpha + \sin\{i\,(\mp\sin P\sin\delta\sin\alpha \mp \cos P\cos\alpha)\}\Big] \tag{2}$$

Here, the $\pm$ refer expected two normal at the projection of galaxy on the celestial sphere. Inclination angle can be obtained using the formula [41].

$$\cos^2 i = \frac{q^2 - q^{*2}}{1 - q^{*2}} \tag{3}$$

The formula is called Holmberg Formula. In this framework, the equation ($q = b/a$) expresses the ratio of the semi-minor axis to the semi-major axis, while (q^*) represents the intrinsic flatness of a galaxy. The intrinsic flatness is influenced by the galaxy's shape, which is in turn affected by the eccentricity of its projected elliptical representation on the celestial sphere and its inclination angle. Here, (α) is the right ascension, (δ) refers to the declination, and (P) indicates the position angle of the galaxy.

To address the selection effects that may distort the shapes of anticipated distribution curves within the galaxy database, the researchers create virtual galaxies, adhering to the methodology established by Aryal & Saurer [42]. The angles θ (polar angle) and ϕ (azimuthal angle) are computed utilizing the Godłowski transformations, which facilitate precise modeling of spatial orientations.
The isotropic distribution curves are obtained from simulations involving an extensive dataset of (10^7) virtual galaxies using MATLAB version R2025b using Equations (1) and (2) in equatorial co-ordinate system. This computational strategy enables a thorough analysis of the intrinsic properties of galaxy distribution while reducing the biases that selection effects might introduce.

2 Method of analysis

In the study, the observed orientations of the galaxies are compared with the isotropic distribution curves for both polar angle (θ) and azimuthal angle (ϕ) using three robust statistical tests to assess the level of alignment and any deviations from isotropy. The tests employed are as follows:

2.1 Chi-Square test

The χ^2 test measures how well a theoretical probability distribution fits a set of data. It provides an objective method to determine whether the observed distribution deviates from the isotropic distribution, as described by Equations (4) and (5) [43].

$$\chi^2_\nu = \frac{\chi^2}{\nu} \tag{4}$$

and

$$\chi^2 = \sum \frac{(N_{oi} - N_{ei})^2}{N_{ei}} \tag{5}$$

In these equations, n represents the number of bins, N_{0i} and N_{ei} denote the observed and expected isotropic distributions, respectively, and ν is the degree of freedom, given by $\nu = n - 1$.

2.2 Fourier test

The Fourier test is a useful tool in this analysis, particularly when the distribution shows slow variations in θ or ϕ, facilitating a deeper understanding of the orientation patterns in the context of the proposed evolutionary models. The expressions for the Fourier coefficients Δ_{11} and Δ_{21} are given in Equations (6) and (7), and their standard deviations, $\sigma(\Delta_{11})$ and $\sigma(\Delta_{21})$, can be obtained using the expressions provided in Equations (8) and (9) respectively [44].

$$\Delta_{11} = \frac{\sum_{k=1}^{n}(N_k - N_{0k})\cos 2\theta_k}{\sum_{k=1}^{n}(N_{0k}\cos^2 2\theta_k)} \tag{6}$$

$$\Delta_{21} = \frac{\sum_{k=1}^{n}(N_k - N_{0k})\sin 2\theta_k}{\sum_{k=1}^{n}(N_{0k}\sin^2 2\theta_k)} \tag{7}$$

$$\sigma(\Delta_{11}) = \left(\sum_{k=1}^{n} N_{0k}\cos^2 2\theta_k\right)^{-\frac{1}{2}} \tag{8}$$

$$\sigma(\Delta_{21}) = \left(\sum_{k=1}^{n} N_{0k}\sin^2 2\theta_k\right)^{-\frac{1}{2}} \tag{9}$$

The amplitude of Fourier coefficient is given by Equation (10):

$$\Delta_1 = \left(\Delta_{11}^2 + \Delta_{21}^2\right)^{1/2} \tag{10}$$

The first order Fourier probability can be calculated by using the corresponding formula along with its standard deviation. The Fourier coefficient is particularly important because it indicates the direction of deviation given by Equation (11).

$$\sigma(\Delta_1) = \left(\frac{2}{nN_0}\right)^{1/2} \tag{11}$$

Δ_{11} is often used as a statistical measure to quantify the alignment of galaxy rotation axes in relation to a defined reference frame, such as a plane that could represent the average orientation of other structures in the universe.

2.3 Autocorrelation test

The autocorrelation test is used to determine if there exists a linear relationship between galaxy orientations in angular bins. Essentially, it examines whether the number of galaxies in one angular bin is related to the number of galaxies in nearby angular bins. This can indicate whether the orientation of one galaxy has some influence on the orientation of others in close proximity.

The auto-correlation function is given by Equation (13), along with its standard deviation in Equation (12).

$$\sigma(\Delta_1) = \sqrt{n} \tag{12}$$

$$C = \sum_{k=1}^{n} \frac{(N_k - N_{0k})(N_{k+1} - N_{0k+1})}{(N_{0k} N_{0k+1})^{1/2}} \quad (13)$$

For isotropic, auto-correlation vanishes, i.e. $C \to 0$ [44].

3 Results and discussion

The following requirements must be satisfied for a distribution to be deemed anisotropic: First-order Fourier coefficient ($\Delta_{11}/\sigma(\Delta_{11})$) larger than 1.5 or less than -1.5, autocorrelation coefficient greater than 1.0 or less than -1.0, chi-square probability less than 0.050, and first-order Fourier probability $P(>\Delta_1)$ less than 0.150. Humps and dips are used to describe local effects in the samples [43,44]. The θ and ϕ distributions are shown in Tables 1 and 2 respectively.

The angular momentum vectors of galaxies tend to be oriented perpendicular to the equatorial coordinate system when the first-order Fourier coefficient ($\Delta_{11}/\sigma(\Delta_{11})$) for θ is significantly negative, whereas a positive value suggests a tendency for the vectors to be parallel. A significant positive value of ($\Delta_{11}/\sigma(\Delta_{11})$) in the ϕ statistics indicates that the angular momentum vector projections of galaxies tend toward the center of the equatorial coordinate system, while a significant negative value shows that these projections tend to orient tangentially with respect to the equatorial coordinate system [45–50].

Table 1: The first column represents name of sample; second column denote number of galaxies. Third, Fourth Fifth and Sixth columns advocate auto-correlation coefficient, Fourier probability, First-order Fourier coefficient and Chi-square probability respectively of polar angle distribution (θ)

Sample	Number of galaxies	$C/C(\sigma)$	$P(>\Delta_1)$	$\Delta_{11}/\sigma(\Delta_{11})$	$P(>\chi^2)$
z01	591	1.2	0.869	0.3	0.118
z02	1396	-0.4	0.982	-0.2	0.211
z03	2983	0.7	0.886	-0.5	0.880
z04	6142	-0.4	0.938	-0.3	0.475
z05	12159	0.3	0.972	0.2	0.422
z06	22024	1.3	0.472	-1.2	0.666
z07	39169	-1.7	0.515	-1.1	0.438
z08	69904	-1.7	0.071	2.2	0.035
z09	104483	2.2	0.197	-1.8	0.102
z10	135214	1.4	0.470	-1.2	0.007
z11	61045	0.2	0.390	-1.3	0.336
z12	10632	2.7	0.005	-3.0	0.009
z13	7215	12.2	0.000	-5.6	0.000
z14	4517	7.6	0.000	-4.0	0.000
z15	2278	1.8	0.105	-1.8	0.755
z16	1599	0.8	0.237	-1.5	0.354
z17	1628	-1.4	0.492	-0.1	0.279
z18	2331	5.9	0.020	-2.7	0.001
z19	2783	8.5	0.000	-5.3	0.000
z20	2359	24.3	0.000	-6.5	0.000
z21	1445	14.9	0.000	-4.3	0.000
z22	371	2.7	0.002	-3.5	0.000

Table 2: The first column represents name of sample; second column denote number of galaxies. Third, Fourth Fifth and Sixth columns advocate auto-correlation coefficient, Fourier probability, First-order Fourier coefficient and Chi-square probability respectively of Azimuthal angle distribution (ϕ)

Sample	Number of galaxies	$C/C(\sigma)$	$P(>\Delta_1)$	$\Delta_{11}/\sigma(\Delta_{11})$	$P(>\chi^2)$
z01	591	-0.2	0.794	-0.3	0.427
z02	1396	0.1	0.400	0.8	0.707
z03	2983	-0.1	0.429	0.9	0.809
z04	6142	-0.9	0.644	0.9	0.544
z05	12159	2.0	0.021	2.7	0.005
z06	22024	2.0	0.017	2.3	0.264
z07	39169	3.9	0.963	3.4	0.033
z08	69904	10.1	0.000	6.8	0.000
z09	104483	7.9	0.000	5.2	0.000
z10	135214	8.7	0.000	5.1	0.000
z11	61045	2.7	0.029	2.7	0.015
z12	10632	0.04	0.544	1.1	0.388
z13	7215	-0.8	0.586	-0.4	0.014
z14	4517	-0.6	0.806	-0.4	0.715
z15	2278	0.3	1.135	0.3	0.596
z16	1599	0.1	0.352	0.7	0.699
z17	1628	-0.2	0.437	1.2	0.240
z18	2331	12.4	0.000	0.1	0.000
z19	2783	15.7	0.000	-0.5	0.000
z20	2359	18.2	0.000	-2.5	0.000
z21	1445	13.1	0.000	-4.6	0.000
z22	371	7.7	0.000	-4.3	0.000

Alongside the statistical tests, the analysis also involves examining the peaks and troughs in the polar (θ) and azimuthal (ϕ) angle distributions. The solid circles with $\pm1\sigma$ error bars illustrate the observed distribution. In the θ-distribution, a peak (or trough) within the smaller θ range ($0^\circ < \theta < 45^\circ$) suggests that the angular momentum vectors of galaxies are more likely to be oriented parallel (or perpendicular) to the equatorial coordinate system. Conversely, a peak (or trough) in the larger θ range indicates that the angular momentum vectors are more often oriented perpendicular (parallel) to the reference coordinate system [43, 44].

In the histogram for the ϕ-distribution, the solid circles with $\pm1\sigma$ error bars also display the observed distribution. The interpretation of peaks and troughs in the ϕ-distribution is more complex than in the θ-distributions [44, 45] because ϕ spans from -90° to $+90^\circ$. A peak in the central eight bins of the histogram indicates a tendency for the projections of the angular momentum vector to direct toward the center of the chosen coordinate system. In contrast, peaks in the first four and last four bins suggest that the vector projections are more likely oriented tangentially with respect to the chosen reference coordinate system.

The examination of the polar (θ) and azimuthal (ϕ) distributions offers important insights into the orientation of angular momentum among galaxies within the z-magnitude range of 12.0 to 12.5, designated as the sample z01, which contains 591 galaxies. Focusing on the θ-distribution, the statistics indicate a chi-square probability $P(>\chi^2) = 0.118$. This relatively high probability suggests that the distribution of polar angles does not significantly differ from isotropy, implying a roughly uniform scattering of the galaxies' angular momentum vectors in this angle range. Furthermore, the auto-correlation coefficient $C/C(\sigma) = 1.2$ strengthens this indication of anisotropy, as a low correlation suggests minimal dependence between the angles of various galaxies. This lack of correlation supports the idea that there is no systematic alignment in the angular momentum orientations among them. Additionally, the first-order Fourier coefficient $\Delta_{11}/\sigma(\Delta_{11}) = 0.3$ and its associated Fourier probability $P(>\Delta_1) = 0.869$, further affirm the conclusion of isotropy. A Fourier probability value near 0.869 implies that any observed variations in the distribution are likely random rather than indicative of a significant underlying pattern.

In conclusion, three statistical indicators for the polar angle distribution within this galaxy sample suggest a largely isotropic arrangement of angular momentum vectors, pointing to a lack of preferential orientation in these vectors within the specified

z-magnitude range.

In Figure 1, for small angles ($\theta \leq 45°$), the number of observed galaxies is 931, while the expected number is 909, meaning there are 22 more observed galaxies than expected. In this region, two humps appear at $\theta = 27.5°$ and $32.5°$ with $< 1\sigma$ error.

For large angles ($45° < \theta < 90°$), the observed and expected numbers of galaxies are 251 and 273, respectively, with 22 less observed galaxies than expected, and 2 dips are observed at $47.5°$ and $45°$, but their values are error.

The first row of Table 2 shows the statistics of the azimuthal angle (ϕ) distribution of galaxies in sample z01. In this sample the value of Chi-square probability $P(> \chi^2)$ is found to be 0.427, the Auto-correlation coefficient $C/C(\sigma)$ is found to be -0.2, the first order Fourier coefficient $\Delta_{11}/\sigma(\Delta_{11})$ is found to be -0.3 and the first order Fourier probability $P(> \Delta_1)$ is found to be 0.794. All these statistics suggest strong isotropy.

In Figure 1, the observed galaxies and expected galaxies in ten central bins are found to be 738 and 744. Thus, the observed galaxies are less than that of expected by 6. In this region, one hump at $5°$ and 2 dips at $-35°$ and $25°$ are observed with . At the outer region, no humps and dips are observed. Hence, no preferred alignment is found to be noticed.

Overall, the galaxies appear randomly distributed, consistent with the Hierarchy model [1].

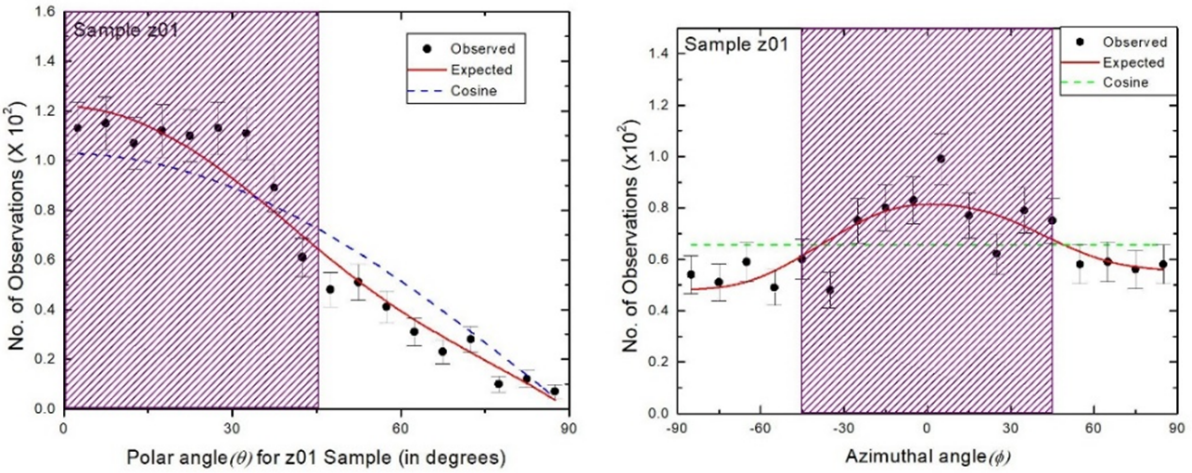

Figure 1: Illustrates the distributions of the polar angle (θ) and the azimuthal angle (ϕ) for galaxies in the z01 sample. The expected distributions are depicted by the solid line, while the observed distribution is represented by the solid circles accompanied by $\pm 1\sigma$ error bars. For comparison, the cosine and average distributions are shown as dashed lines.

Similar results are obtained samples z02, z03, z04, z05, z11, and z16 for polar angle distribution and z02, z03 z04, z12, z13, z14, z15, z16, and z17 for azimuthal angle distribution. These statistics indicate strong isotropy [**?**]. Controversial results are seen for z05 and z11 samples that is polar angle distribution shows isotropy but azimuthal angle advocates anisotropy. The results are due choose of reference co-ordinate system [44].

For the samples z06, z07, z19 and z17 we observed isotropy indicated by all statistical except autocorrelation coefficient in polar angle distribution. This is due to binning effect; the effect can be solved by re-binning. First order fourier coefficient is main test of galaxy orientation and hence we mainly focus on the statistical test [43].

Now we want to explain the results of sample z08 of z-magnitude range of 15.5 to 16.0 for the polar (θ) which contains 69,904 galaxies. Focusing on the θ-distribution, the statistics indicate a chi-square probability $P(> \chi^2) = 0.035$,autocorrelation coefficient $C/C(\sigma) = -1.7$, the first-order Fourier coefficient $\Delta_{11}/\sigma(\Delta_{11}) = 2.2$ and its associated Fourier probability $P(> \Delta_1) = 0.071$.

The ninth row of Tables 2 shows the statistics of the azimuthal angle (ϕ) distribution of galaxies in sample z08. In this sample the value of Chi-square probability $P(> \chi^2)$ is found to be 0.000, the Auto-correlation coefficient $C/C(\sigma)$ is found to be 10.1,

the first order Fourier coefficient $\Delta_{11}/\sigma(\Delta_{11})$ is found to be 6.8 and the first order Fourier probability $P(> \Delta_1)$ is found to be 0.000. All these statistics suggest strong anisotropy for polar and azimuthal angle.

In Figure 2, for small angles ($\theta \leq 45°$), the number of observed galaxies is 105320 while the expected number is 104765, meaning there are 555 more observed galaxies than expected. For large angles ($45° < \theta < 90°$), the observed and expected numbers of galaxies are 34488 and 35042, respectively, with 554 less observed galaxies than expected. Due to very large number of observations humps and dips are not observed clearly.

In Figure 2, the observed galaxies and expected galaxies in ten central bins in azimuthal angle distribution are found to be 86,844 and 85,787 i.e. 1057 more observed values than expected. In this region, continuous humps are seen at 5°, 15° and 25°. All statistics, number of observations and humps suggest that projection of spin vectors are toward center of co-ordinate system.

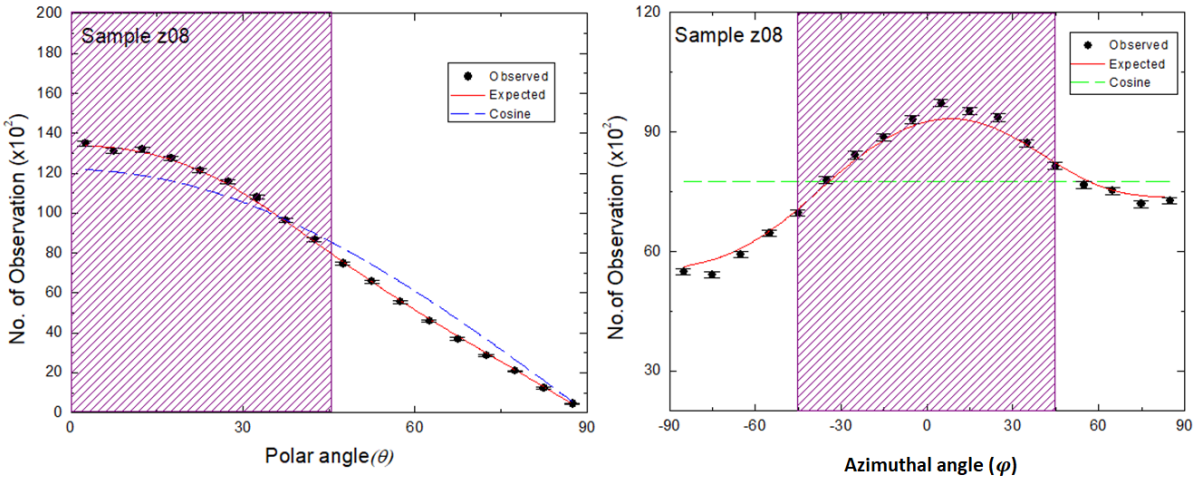

Figure 2: Illustrates the distributions of the polar angle (θ) and the azimuthal angle (ϕ) for galaxies in the z08 sample. The expected distributions are depicted by the solid line, while the observed distribution is represented by the solid circles accompanied by $\pm 1\sigma$ error bars. For comparison, the cosine and average distributions are shown as dashed lines.

We now examine the polar (θ) and azimuthal (ϕ) distributions of galaxies with z-magnitudes in the range 17.5 to 18.0 of sample z12. There are 10,632 observations. The thirteenth row of Table 1 presents the statistics for the polar angle (θ) distribution of the sample. The values are as follows: chi-square probability $P(> \chi^2) = 0.009$, autocorrelation coefficient $C/C(\sigma) = 2.7$, first-order Fourier coefficient $\Delta_{11}/\sigma(\Delta_{11}) = -3.0$, and first-order Fourier probability $P(> \Delta_1) = 0.005$. A negative value of $\Delta_{11}/\sigma(\Delta_{11})$ indicates that the spin vectors of galaxies tend to be oriented perpendicular to the equatorial coordinate system. These statistics suggest anisotropy.

In Figure 3, for small angles ($0° < \theta < 45°$), the observed number of galaxies is 16,103, while the expected number is 16,289, indicating 186 less observed galaxies than expected. In this region, one significant dip is seen at 17.5° having 1.5σ error. For large angles ($45° < \theta < 90°$), the observed and expected numbers are 5,161 and 4,974, respectively, with no significant humps or dips. Also, first order coefficient, $\Delta_{11}/\sigma(\Delta_{11}) = -3.0$ indicates that spin vector is perpendicular to reference coordinate system which supports Primordial Vorticity model.

The thirteenth row of Tables 2 presents the statistics for the azimuthal angle (ϕ) distribution for sample z12. Here, $P(> \chi^2) = 0.388$, $C/C(\sigma) = 0.04$, $\Delta_{11}/\sigma(\Delta_{11}) = 1.1$, and $P(> \Delta_1) = 0.544$, indicating isotropy.

In Figure 3, for $\phi \approx \pm 45°$, the observed number of galaxies in the ten central bins is 13,006, while the expected number is 12,889 meaning 117 more galaxies are observed than expected. In this region, one hump is observed at 15° ($< 1.0\sigma$). In the outer region, one dip is observed at 55° ($< 1.0\sigma$).

In sample z12, the result of polar angle (θ) distribution suggest anisotropy and azimuthal angle (ϕ)

distribution suggest isotropy giving mixed result, this is due to reference co-ordinate system. In this case we consider the polar angle distribution [44].

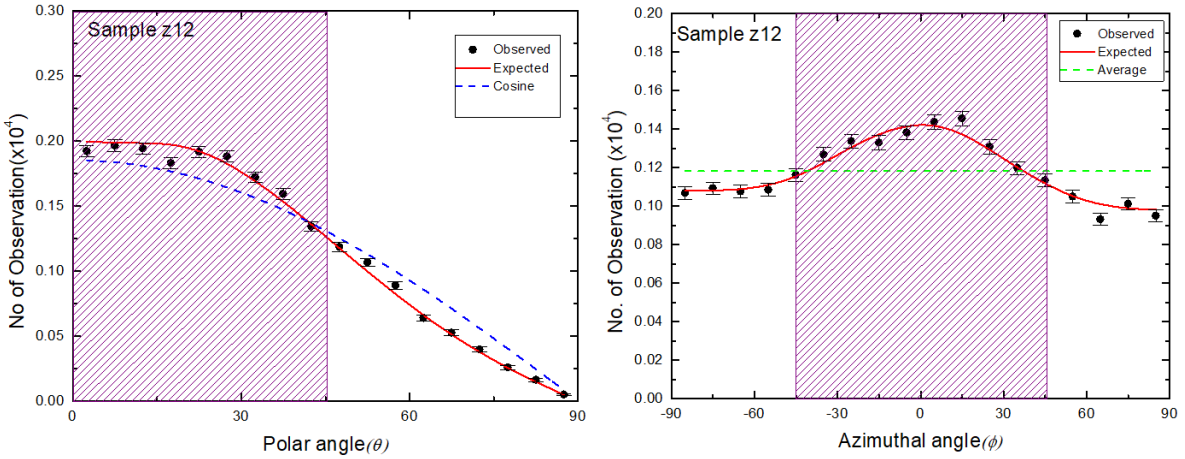

Figure 3: Illustrates the distributions of the polar angle (θ) and the azimuthal angle (ϕ) for galaxies in the z12 sample. The expected distributions are depicted by the solid line, while the observed distribution is represented by the solid circles accompanied by $\pm 1\sigma$ error bars. For comparison, the cosine and average distributions are shown as dashed lines.

The 21st row of Tables 2 presents the statistics for the polar angle (θ) distribution for sample z20. Here, $P(> \chi^2) = 0.000$, $C/C(\sigma) = 24.3$, $\Delta_{11}/\sigma(\Delta_{11}) = -6.5$, and $P(> \Delta_1) = 0.000$, indicating highly anisotropy.

In Figure 4, for small angles ($0° < \theta < 45°$), the observed and expected number of galaxies are 3,304 and 3,535 indicating 231 less observed galaxies than expected. In this region, five dips are seen at 7.5°, 17.5°, 27.5°, 32.5° and 37.5°. For large angles ($45° < \theta < 90°$), the observed and expected number of galaxies are 1414 and 1182 indicating 232 more observed than expected. In this region, five humps are observed at 62.5°, 67.5°, 72.5°, 77.5° and 82.5°.

All statistics and graphical analysis suggest that the spin vector of galaxies tend to perpendicular to the plane of the coordinate system, supporting Primordial Vorticity Theory.

The 21st row of Table 2 presents the statistics for the azimuthal angle (ϕ) distribution for sample z20. Here, $P(> \chi^2) = 0.000$, $C/C(\sigma) = 18.2$, $\Delta_{11}/\sigma(\Delta_{11}) = -2.5$, and $P(> \Delta_1) = 0.000$, indicating also anisotropy. In Figure 5, for $\phi \approx \pm 45°$, the observed number of galaxies in the ten central bins is 2825, while the expected number is 2895, meaning 70 less galaxies are observed than expected. In this region, one dip is observed at 35° ($< 1.0\sigma$). In the outer region, four humps are observed at $-85°$, $-75°$, $-65°$, $-55°$, and four dips are observed at 55°, 65°, 75°, 85° ($< 1.5\sigma$). All statistics and graphical analysis advocates that spin vector projection is tangent to the reference plane.

4 Conclusion

We have studied the spatial orientation of 492,268 z-magnitude galaxies surveyed by SDSS, with redshifts in the range 0.010 to 0.150, with respect to the equatorial coordinate system. The z-magnitudes were observed using a 8932Å Charged Coupled Device (CCD) filter attached to the SDSS telescope located in New Mexico, USA. Using the "position angle–inclination" method, we converted two-dimensional parameters into three-dimensional galaxy rotation axes, as indicated by Flin & Godlowski [40]. To understand the theoretical isotropic distribution of galaxy rotation axes and mitigate selection effects, we performed random simulations by generating 10^7 virtual galaxies based on Aryal & Saurer [42]. Differences between observed and theoretical distributions were analyzed using chi-square, auto-correlation, and Fourier analysis [51–53]. This study aimed to explore non-random effects in galaxies and evaluate the suitability of the coordinate system for representing the true orientations of distant galaxies [54]. Our observations led to the following conclusions:

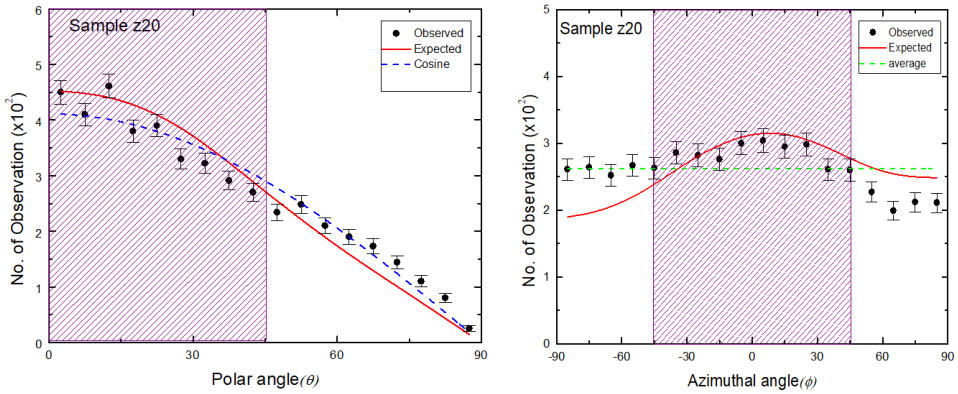

Figure 4: Illustrates the distributions of the polar angle (θ) and the azimuthal angle (ϕ) for galaxies in the z20 sample. The expected distributions are depicted by the solid line, while the observed distribution is represented by the solid circles accompanied by $\pm 1\sigma$ error bars. For comparison, the cosine and average distributions are shown as dashed lines.

1. First order fourier coefficient as well as graphical analysis of the samples z01, z02, z03, z04, z05, z06, z07, z10, z11, z16, and z17 suggest that the polar angle distributions are isotropic i.e. spin vectors are randomly oriented. These results support the Hierarchy model [1].

2. First order fourier coefficient as well as graphical analysis of the samples z09, z12, z13, z14, z15, z18, z19, z20, z21, and z22 suggest that the polar angle distributions are anisotropic i.e. spin vectors are perpendicularly oriented. These results support the Primordial Vorticity Model [25, 55, 56].

3. First order fourier coefficient as well as graphical analysis of the samples z01, z02, z03, z04, z12, z13, z14, z15, z16, z17, z18 and z19 suggest that the azimuthal angle distributions are isotropic i.e. spin vectors are randomly oriented.

4. First order fourier coefficient as well as graphical analysis of the samples z05, z06, z07, z08, z09, z10, and z11 suggest that the azimuthal angle distributions are anisotropic i.e. spin vectors projections toward the center of equatorial coordinate system.

5. First order fourier coefficient as well as graphical analysis of the samples z20, z21, and z22 suggest that the azimuthal angle distributions are anisotropic i.e. spin vectors projections tangential to the equatorial coordinate system.

6. First order fourier coefficient as well as graphical analysis of the sample suggest that the polar angle distributions are anisotropic i.e. spin vectors are parallel oriented. These results support the Pancake Model [3, 57].

7. Overall, no global preferred alignment is observed in the spatial orientation of galaxy spin vectors, suggesting consistency with the Hierarchy model. However, local effects are observed in most samples, which may indicate tidal interactions between rotation axes or the merging process, affecting the angular momentum vectors of some galaxies.

8. Humps and dips in the angular momentum distributions are observed in different samples, caused by local effects. These features likely correspond to density fluctuations at local scales in deep fields.

9. To study non-random effects in galaxy orientation, the equatorial coordinate system was used as a physical reference. The Hierarchy model predicts that the choice of coordinate system does not alter preferred alignments, while the Pancake model emphasizes the importance of a physical reference system. Our results show a mixture of both models across different samples. To further investigate, other systems such as the Galactic or Super galactic coordinates were also considered.

10. The random simulations were carried out on a PC with 4 GB of RAM, generating 10^7 virtual galaxies. In the future, we plan to simulate 10^8 virtual galaxies to obtain smoother and more precise isotropic distribution curves.

Acknowledgements

We would like to thank the Sloan Digital Sky Surveys (SDSS), Central department of physics, Tribhuvan University, Professor Dr. Narayan Prasad Adhikari, Dr. Kishori Yadav and Mr. Bisnu Bist.

References

[1] Peebles PJE. Origin of the angular momentum of galaxies. The Astrophysical Journal. 1969;155:393-401.

[2] Sunyaev RA, Zeldovich YB. Formation of clusters of galaxies; protocluster fragmentation and intergalactic gas heating. Astronomy and Astrophysics. 1972;20:189.

[3] Doroshkevich AG. The origin of rotation of galaxies. The Astrophysical Journal. 1973;14:11-3.

[4] Shandarin SF. Orientation of angular momenta of galaxies. Soviet Astronomy. 1974;18:392-3.

[5] Dekel E. An axiomatic characterization of preferences under uncertainty: Weakening the independence axiom. Journal of Economic Theory. 1986;40(2):304-18.

[6] Efstathiou G, Silk J. The formation of galaxies. Fundamentals of Cosmic Physics. 1983;9.

[7] Shandarin S, Habib S, Heitmann K. Cosmic web, multistream flows, and tessellations. Physical Review D. 2012;85(8):083005.

[8] Giahi-Saravani A, Schäfer BM. Weak gravitational lensing of intrinsically aligned galaxies. Monthly Notices of the Royal Astronomical Society. 2014;437(2):1847-57.

[9] Silk J. When were galaxies and galaxy clusters formed? Nature. 1968;218(5140):453-4.

[10] Peebles PJ, Yu JT. Primeval adiabatic perturbation in an expanding universe. The Astrophysical Journal. 1970;162:815.

[11] Sunyaev RA, Zeldovich YB. Small-scale fluctuations of relic radiation. Astrophysics and Space Science. 1970;7(1):3-19.

[12] Garbaczewski P, Stephanovich V. Levy flights in confining potentials. Physical Review E. 2009;80(3):031113.

[13] Garbaczewski P, Stephanovich V, Kedzierski D. Heavy-tailed targets and (ab) normal asymptotics in diffusive motion. Physica A. 2011;390:990-1008.

[14] Peebles PJE. Fluid dark matter. The Astrophysical Journal. 2000;534(2):L127.

[15] Yadav SN, Aryal B, Saurer W. Preferred alignments of angular momentum vectors of galaxies in six dynamically unstable Abell clusters. Research in Astronomy and Astrophysics. 2017;17(7):064.

[16] Schäfer BM, Merkel PM. Galactic angular momenta and angular momentum couplings in the large-scale structure. Monthly Notices of the Royal Astronomical Society. 2012;421(4):2751-62.

[17] Catelan P, Theuns T. Non-linear evolution of the angular momentum of protostructures from tidal torques. Monthly Notices of the Royal Astronomical Society. 1996;282(2):455-69.

[18] Lee J, Pen UL. Detection of galaxy spin alignments in the point source catalog redshift survey shear field. The Astrophysical Journal. 2002;567(2):L111.

[19] Sah SSP, Yadav SN. Study preferred alignments of angular momentum vector of i–magnitude SDSS galaxies having redshift 0.54–0.60. BIBECHANA. 2022;19(1-2):68-74.

[20] Hoyle F. Problems of cosmological areodynamics. In: Proceedings of a Symposium on Motion of Gaseous Masses of Cosmical Dimensions; 1951. p. 195.

[21] White SD. Angular momentum growth in protogalaxies. Astrophysical Journal. 1984;286:38-41.

[22] Kiessling W, Schobben M, Ghaderi A, Hairapetian V, Leda L, Korn D. Pre-mass extinction decline of latest Permian ammonoids. Geology. 2018;46(3):283-6.

[23] von Weizsäcker CF. The evolution of galaxies and stars. The Astrophysical Journal. 1951;114:165-86.

[24] Gamow G. The role of turbulence in the evolution of the universe. Physical Review. 1952;86:251-60.

[25] Ozernoy LM. Whirl theory of the origin of galaxies and clusters of galaxies. In: The Large Scale Structure of the Universe. vol. 79. IAU Symposium; 1978. p. 427.

[26] Gamow G. Expanding universe and the origin of elements. Physical Review. 1946;70(7-8):572.

[27] Godel K. An example of a new type of cosmological solutions of Einstein's field equations of gravitation. Reviews of Modern Physics. 1949;21(3):447.

[28] Collins CB, Hawking SW. Why is the universe isotropic? Astrophysical Journal. 1973;180:317-34.

[29] Godłowski W. Global and local effects of rotation: Observational aspects. International Journal of Modern Physics D. 2011;20(09):1643-73.

[30] Paulus PB, Larey TS, Ortega AH. Performance and perceptions of brainstormers in an organizational setting. Basic and Applied Social Psychology. 1995;17(1-2):249-65.

[31] Mo KC, Chelliah M, Carrera ML, Higgins RW, Ebisuzaki W. Atmospheric moisture transport over the United States and Mexico as evaluated in the NCEP regional reanalysis. Journal of Hydrometeorology. 2005;6(5):710-28.

[32] Bower GC, Goss WM, Falcke H, Backer DC, Lithwick Y. The intrinsic size of Sagittarius A* from 0.35 to 6 cm. The Astrophysical Journal. 2006;648(2):L127.

[33] Heavens A, Peacock J. Tidal torques and local density maxima. Monthly Notices of the Royal Astronomical Society. 1988;232(2):339-60.

[34] Hwang HS, Lee MG. Searching for rotating galaxy clusters in SDSS and 2dFGRS. The Astrophysical Journal. 2007;662(1):236.

[35] Noh Y, Lee J. The alignments of disk galaxies with the local pancakes. arXiv preprint astro-ph/0602575. 2006.

[36] Li LX. Effect of the Global Rotation of the Universe on the Formation of Galaxies. General Relativity and Gravitation. 1998;30(3):497-507.

[37] Godlowski W, Szydlowski M, Flin P. Some remarks on the angular momenta of galaxies, their clusters and superclusters. General Relativity and Gravitation. 2005;37(3):615-25.

[38] Birch P. Is the universe rotating? Nature. 1982;298(5873):451-4.

[39] Pallathadka GA, et al. Double White Dwarf Binaries in SDSS-V DR19: A catalog of DA white dwarf binaries and constraints on the binary population. arXiv preprint arXiv:250902906. 2025.

[40] Flin P, Godlowski W. The orientation of galaxies in the Local Supercluster. Monthly Notices of the Royal Astronomical Society. 1986;222(3):525-41.

[41] Holmberg E. On the apparent diameters and the orientation in space of extragalactic nebulae. Lunds Astronomical Observatory Meddelanden. 1946;117:3-82.

[42] Aryal B, Saurer W. Comments on the expected isotropic distribution curves in galaxy orientation studies. Astronomy and Astrophysics. 2000;364:L97-L111.

[43] Godlowski W. Some aspects of the galactic orientation within the local supercluster. Monthly Notices of the Royal Astronomical Society. 1994;271:19-30.

[44] Godlowski W. Galactic orientation within the local supercluster. Monthly Notices of the Royal Astronomical Society. 1993;265:874-80.

[45] Aryal B. Spatial orientation of spin vectors of galaxies in 42 Abell clusters. University of Innsbruck; 2002.

[46] Aryal B, Saurer W. The influence of selection effects on the isotropic distribution curve in galaxy orientation studies. ASP Conference Series. 2001;230:A145-54.

[47] Aryal B, Saurer W. Spin vector orientations of galaxies in eight Abell clusters of BM type I. Astronomy and Astrophysics. 2004;425:871-9.

[48] Aryal B, Saurer W. Spin vector orientations of galaxies in seven Abell clusters of BM type III. Astronomy and Astrophysics. 2005;432:841-31.

[49] Aryal B, Saurer W. Morphological dependence in the spatial orientations of local supercluster galaxies. Astronomy and Astrophysics. 2005;432:431-9.

[50] Aryal B, Saurer W. Spin vector orientation of galaxies in the region 15h48m (2000) 19h28m, -68 (2000) -62. Monthly Notices of the Royal Astronomical Society. 2005;360:125-35.

[51] Yadav SN, Sah SK. Study of spatial orientation of angular momentum of z-magnitude SDSS DR-13 galaxies. Journal of Institute of Science and Technology. 2021;26(1):1-7.

[52] Yadav SN, Aryal B, Saurer W. A study of coexistence between the Hubble flow and the random alignments of spin vectors of SDSS galaxies. BIBECHANA. 2015;12:114-27.

[53] Yadav SN. A study of z-magnitude dependence in the spatial orientation of angular momentum vectors of galaxies. Tribhuvan University Journal. 2016;30(2):195-210.

[54] Aryal B, Yadav SN, Saurer W. Spatial orientation of galaxies in the Zone of Avoidance. Bulletin of the Astronomical Society of India. 2012;40:65.

[55] Ozernoy LM. Whirl theory of the origin of galaxies and clusters of galaxies. IAU Symposium. 1974;63:227-40.

[56] Stein R. Galaxy formation from primordial turbulence. Astronomy and Astrophysics. 1974;35:17-29.

[57] Doroshkevich AG, Shandarin SF, Saar E. Spatial structure of protoclusters and the formation of galaxies. Monthly Notices of the Royal Astronomical Society. 1978;184:643-60.